Development of copper matrix composites reinforced by alumina and carbon materials via synergic milling

Adolfo José de Melo Chinopa de Sousa Ribeiro
adolfo.ribeiro@tecnico.ulisboa.pt

Instituto Superior Técnico, Universidade de Lisboa, Portugal

October 2020

Abstract

Copper based composites are used for several thermo-electric applications. However, low strength, contaminant sensitivity and low service temperatures limit both applications and production methods. The development of a manufacturing method capable of providing a stronger copper matrix, with higher thermal stability, while minimizing transport property loss is imperative.

Graphite and alumina particles have been used to produce copper composites with improved dispersion strengthening and thermal stability. To increase matrix strength and copper recrystallization temperature silver was also added: the combined effect of these properties fosters milling efficiency.

This work approaches the production of 2wt% alumina, 2wt% graphite reinforced copper matrix composites, with or without 1.6wt% silver addictions, via high energy milling. The synergistic use of copper for milling media constitutes a paradigm shift in contrast to previously used media that emphasised high hardness as the optimal choice.

5 gram powder batches were milled up to 8 hours, at 200 RPM, in argon. A minimum copper crystallite size, as determined by XRD, of 21nm, 18nm and 20nm were respectively obtained for the Copper-Graphite, Copper-Graphite-Alumina and Copper-Graphite-Alumina-Silver systems. The maximum obtained ultra-microhardness values, HV0.025, were respectively 199±18, 220±27 and 221±8. Silver addition increased powder mass yield from 21% to 56% for 8 hours milling, providing an answer to losses by powder welding to the milling media.

Keywords: Copper; Nanocomposite; mechanical alloying; Alumina; Graphite; Silver

1. Introduction

Copper engineering applications, from household computer heat sinks to first wall panel heat sinks in nuclear fusion devices, rely on its mechanical, corrosion and thermal and electrical transport properties [1]. However high temperature performance is always a concern due to grain growth and recovery [2] with copper displaying a recrystallization temperature as low as 360K [3]. This effect severely impacts applications of copper heat sinks and contactors, by requiring a reduction of service temperatures, and is incompatible with the high operation temperatures required for fusion reactors application [4] and resistance spot welding [5].

This thesis aims at: producing Copper based Metallic Matrix Composites, MMC with reinforcing phases of graphite, alumina and silver, increasing room temperature, service temperatures, hardness, reducing wear and friction coefficients while retaining good transport properties; employing of the synergic milling approach to reducing contamination during the milling process and tackling of inherent challenges of this method.

2. State-of-the-Art

2.1. Copper – Graphite system

Graphite has low thermal expansion coefficient, high corrosion resistance, good electrical conductivity, and lubricating properties. The main benefit of adding graphite to an MMC is the establishment of a graphite rich tribo-layer that allows the decrease of the wear coefficient, leading ultimately to the decrease of the wear rate. Finely subdivided small graphite crystallites provide a more effective wear behaviour, as edge surfaces are more chemically active binding readily with the atmospheric gas environment molecules [6,7].

Overall the incorporation of graphite decreases the composite's yield strength, hardness, and the friction and wear coefficients of copper [8]. It also slightly decreases thermal and electrical conductivity [9].

2.2. Copper – Graphite – Alumina system

Copper alumina composites are the most common oxide dispersed reinforced copper matrix composites [10,11]. Alumina particles act as a suitable physical reinforcement for the matrix due to its high hardness and thermal stability. Dispersed oxide particles provide and obstacle to dislocation motion increasing strength. Simultaneously oxide particles will pin grain boundaries preventing grain growth during high temperature work. The addition of alumina will decrease electrical conductivity, with the amount of alumina and respective particle size and dispersion being the most important factors.

2.3. Copper – Graphite -- Alumina – Silver system

Small additions of silver have been added to copper forming solid solutions to increase recrystallization temperature and hardness via solid solution hardening. [12–15]. Small additions of silver, <0.3wt%, don't decrease copper conductivity bellow 99,5% IACS [14,16]. These properties are relevant not only to material performance, but to the success of mechanical alloying by stopping recovery mechanisms during milling.

2.4. Thoughs on mechanical milling

Mechanical Milling is a powder processing technique that uses the motion of milling balls against powder particles to enable the production of powder materials by milling elemental powders [17]. Both powder size and crystallite size are refined during milling, through different mechanisms:

Work hardened powders will fracture leading to a decrease in powder size. However, powders are also subjected to recrystallization, enabled by the temperature increase during milling which will offset the work hardening effect, and to cold welding leading to an increase in powder size.

Crystallite size is refined through continuous deformation. Milling creates a high dislocation density. The arrangement of dislocations will form low angle boundaries within the grain, which rotate into high angle boundaries and eventually restart the process when these sub grains start pilling up dislocations. The theorical minimum crystallite size would be one that cannot sustain a dislocation pile up [18], However the experimental minimum, depends on the competition between dislocation pile up and recovery mechanisms [19].

The reduction of lamellar thickness, continuous welding, creation of new surfaces along fractured powders, increase in dislocation density and temperature rise enables an increase the diffusion kinetics and imultaneously extends the solid solubility of the system.

The same mechanism that renders alloying possible, will facilitate the incorporation of contaminats from the milling environment into the powder. Control of the milling atmosphere and purity of elemental powders are two methods of eliminating sources of contamination.

However, incorporation of milling media debris into the powders is very difficult to prevent, as the same attrition and collision forces responsible for the fracture of powder particles are acting on the vial walls and balls. Using harder materials to reduce the amount of wear is seldom a satisfying solution, because it restricts the range of available powders and the milling media often outweighs the milled powder in a high proportion, so even small amount of mass loss from the milling media will lead to high contamination of the powder.

The most successful approach to minimize the contamination of milled powder requires a paradigm shift from reducing the amount of milling media wear to reduce the impact of contamination. The Synergistic Milling approach used in this work employs milling media of the same material as the powder mixture to eliminate the contamination of milling powders with foreign elements.

3. Experimental Procedure

Electrolytic copper w (99,7%, ~63μm, Pometon), synthetic graphite powders (99.6%, ~2.4 μm, Timrex KS4 grade), alumina powders (99.8%, ~0.5 μm, Almantis CT3000SG grade) and silver powders (99.9%, ~3 μm, Sigma-Aldrich 327085 Silver grade) were used as starting materials.

Ball milling experiments of the Copper–Graphite systems were carried out with different milling rates (200,400 and 550RPM). The Copper–Graphite–Alumina and Copper–Graphite–Alumina–Silver experiments were all milled at a fixed milling rate of 200RPM 15m, 30m, 1h and 8h effective milling cycles, in an argon atmosphere. 30 minute interval stops were made every 30 minutes for cooling

Batches with approximately 5g of elemental powders were milled. 100mg of graphite (Cg), 100mg of alumina and 80 mg of silver were added as needed. No process control agent (PCA) was used. The ball-to-powder ratio was kept at 10:1. Experiments were conducted on a Retsch PM100 planetary ball mill using a 250mL prototype ETP copper vial loaded with 5mm ETP copper milling balls. Powder loading into the vial was carefully controlled inside a glove box (MBraun Unilab Plus) with dry Argon atmosphere

(<0.1ppm H_2O and O_2). The vial was closed inside the glove box with an airtight security hatch to ensure inert atmosphere during processing and afterward. The vial was only opened again once back inside the glove box.

A JEOL field emission gun scanning electron microscope model JSM-7001F equipped with an Oxford Light Elements EDS Detector was used to study the Cu-Cg powder system morphology.

Samples were hot mounted in a conductive resin, grinded and polished, with the last step of polishing using a custom-made OPS.

XRD diffractograms were obtained using an acquisition time of 0.5 seconds and step size of 2Θ=0.5º were used. Scans were carried out from 2Θ=20º to 2Θ =100º for all samples. Additionally, more time consuming but accurate measurements were carried out over smaller intervals when suitable.

Raman spectroscopy was performed in order to characterize graphite structure evolution. A confocal Raman spectrometer, Horiba Jobin-Yvon HR Evolution, with a 532 nm laser, and a 100× objective was used to collect the spectra. 5 accumulations and 10 s acquisition were collected for each spectrum. The software FITYK 0.9.8 was used for background removal.

Nanoindentation tests were performed using a Shimadzu DUH-211S dynamic ultramicrohardness tester using a load of 25 mN, a load increase rate of 4.4413mN/s and a dwell time at maximum load of 15 s.

Milled powders and milling balls were weighed after each milling cycle in order to characterize process yield and powder mass flow.

4. Results

4.1. Powder mass yield

Copper powders tend to cold weld together, increasing powder size. This effect was reported for pure copper milling under air and protective atmosphere [20], during milling with carbon reinforcement [21] and during milling with alumina reinforcement [22].

However, no powder mass loss has been reported due to copper welding to the steel milling media, this effect appears to be exclusive to synergic milling experiments. Copper powders will weld to the milling media if the powder material is the same as the milling media, decreasing the process efficiency.

High milling rates, equal or above 400 RPM, were not viable due to negligible mass yield. Figure 1 shows how milling experiments carried out in the Cu-Cg system, at 400 RPM and 600 RPM deliver very low mass yield even for 2h experiments.

Long milling times are necessary to provide the energy from ball impacts enabling the designed structural, morphological, and compositional changes in the powder; however long milling times also lead to a decrease in powder mass yield. Therefore, reduction of mass yield is a chief concern when milling ductile powders, especially for longer milling times.

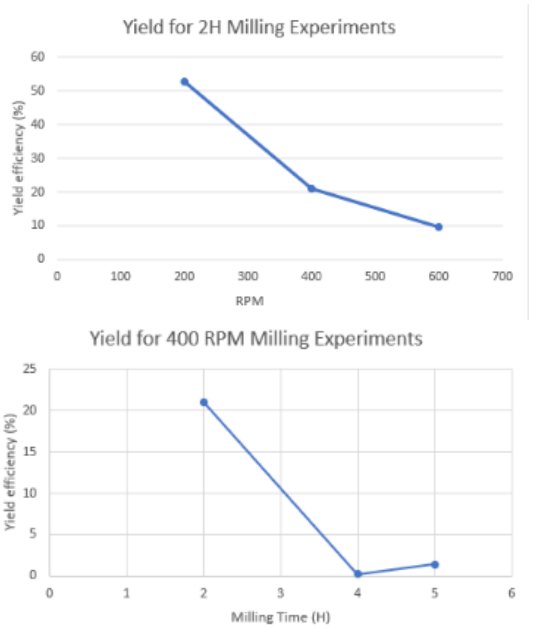

Figure 1 - Powder Mass Yield for different Milling Experiments. Top) For different milling rates; Bottom) for different effective milling time in the Cu-Cg system

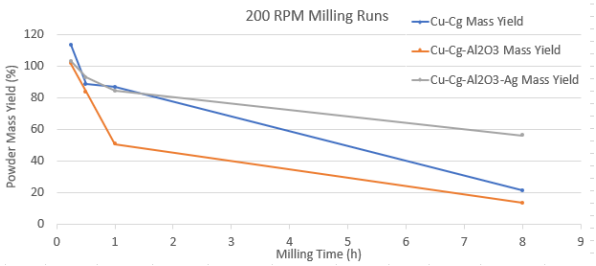

Figure 2 - 200 RPM Milling run over the different powder systems

Different approaches were used to increase milling mass yield. Figure 2; presents the mass yield results for the tested systems and milling cycles.

The increase of strain hardening and decrease of powder ductility to increase fracture was the main strategy used. In the scope of the experiments carried out the 2wt% addition of alumina was not effective to increase the powder mass yield of the Cu-Cg-Al_2O_3 system versus the alumina free Cu-Cg system. The opposite was observed and a decrease in mass yield for all milling times is reported. However, improvements to the powder mass yield were present after the

addition of 1.6wt% silver, due to its effect on copper recrystallization temperature. A measured 260% yield increase, relative to those achieved in other systems for the 8h experiments. Moreover, this increase in efficiency is most intense for longer milling times, which are the critical cycles concerning mass yield decrease.

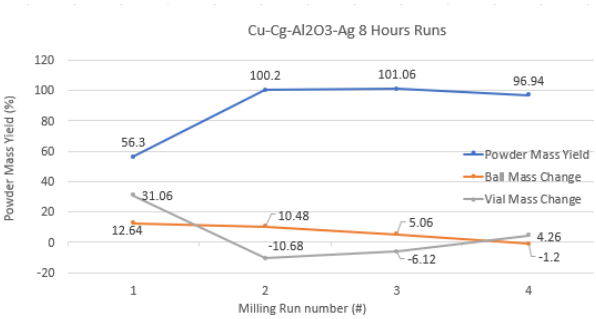

Figure 3 – Powder mass yield in repeated runs in the Cu-Cg-Al_2O_3-Ag, 8h, 200 RPM.

Figure 3 reports that repeated runs, performed in a vial with cumulative coating from previous cycles, featured an increased efficiency. As seasoning a vial was shown to decrease the amount of contamination in regular mechanical milling by coating the milling media with welded powder [19], the repeated experiments show that seasoning a vial is an effective method for increasing the process efficiency.

The use of silver alloying in Cu-Cg-Al_2O_3-Ag system, in tandem with a seasoned vial, has shown to increase the process mass yield to 100%.

4.2. Raman Spectroscopy

The increase in peak G (1300 cm^{-1}) and D (1580 cm^{-1}) peak intensity ratios is indicative of the initial stages of graphite amorphization [23–25]. However, amorphous graphite features a single broad band instead of the sharp G and D peaks, which is absent from the current Raman spectra, according to Figure 5.

As milling time increases, the D peak increases both in intensity and width, while the G peak becomes increasingly smaller and broader. The D/G peak intensity ratio illustrated in Figure 4, reports that most of the graphite defect content develops during the first hour of milling, and the amount of defects within graphite seem to evolve towards an asymptotic maximum, which is reached after one hour of milling for most systems.

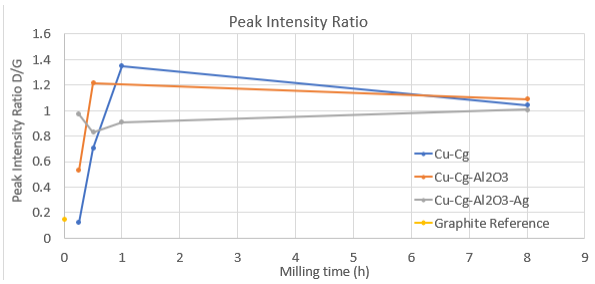

Figure 4- Evolution over milling time of the relative D/G peak intensity ratio.

The increase in graphite edge defect content suggests the increasing presence of finely subdivided small graphite crystallites. Smaller graphite crystallites provide a more effective contact wear behaviour, as edge surfaces are more chemically active, binding to atmospheric gases, improving graphite rich tribolayer lubricating properties [6,7]. Mechanical milling should provide increased wear properties of the copper composite through the decrease in graphite crystallite size.

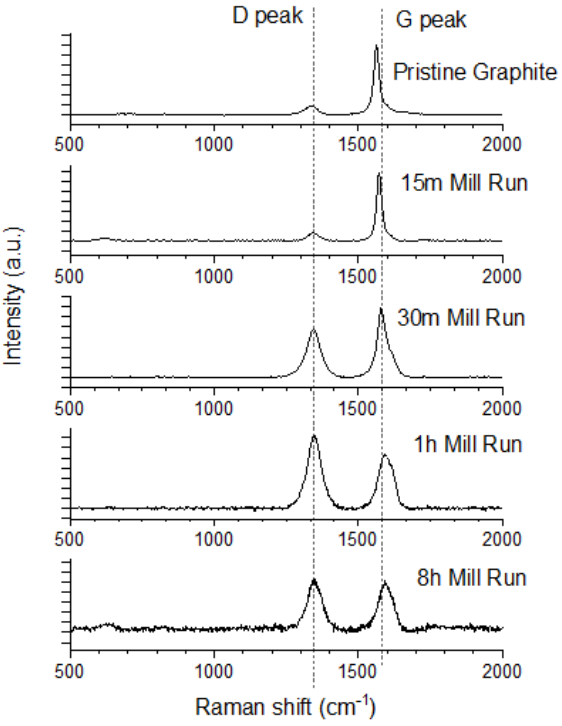

Figure 5 - Raman spectra for un-milled and milled graphite in the Copper Graphite composite system. G and D peaks are highlighted.

4.3.1. XRD - Crystallite size evolution

Figure 6 illustrates the evolution of crystallite size over time in all the milling systems, as well as a pristine sample for comparison. Crystallite size

decrease in different composite systems is negligible, as all observed systems present the same trends.

Crystallite size decrease over milling time indicates that the milling process is most efficient during the early stages of milling. Featuring a decrease from approximately 60nm to approximately 28nm in the first 15 minutes. While the next 8 hours of milling can only reduce the crystallite size to approximately 20nm. Most surprisingly, silver alloying doesn't enable smaller crystallite sizes compared to the un-alloyed powders. This change is unexpected as the addition of silver increases copper recrystallization temperature, this effect is directly related to a decrease in crystallite size for milled Copper [26–28]

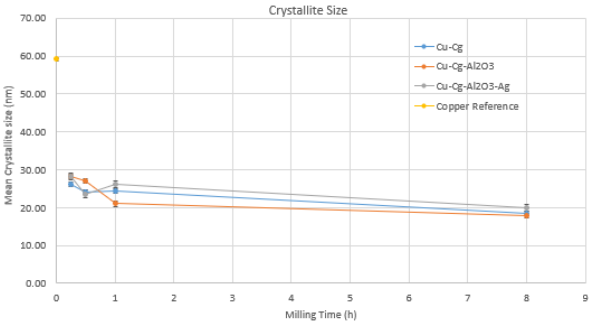

Figure 6- Copper mean crystallite size evolution over milling time via Scherrer analysis. The crystallite size for the pristine copper powders is indicated

4.3.2. XRD - Solid Solution

Lattice parameter shifts indicate the occurrence of solid solution, as foreign atoms are introduced into the copper structure.

The silver system features a linear increase along time as per Figure 7. However, the increase in lattice parameter still fits inside the method's inherent error. The reason for the lattice parameter limited increase is an inherent consequence of the powder composition: an addition of 1at% silver can only provide a proportional lattice parameter shift. Using Vergard's law [29,30] it is possible to estimate the maximum lattice parameter that is achievable for high milling times. Even this calculated value, 0.36196 nm, falls within the method's error.

Even without a lattice parameter shift wide enough to be expressed over the method's inaccuracy, the linear increase of the lattice parameter along milling time and the change in powder mass loss behaviour indicate that the addition of silver to the powder batch does in fact affect the copper powder behaviour. Further suggesting the occurrence of solid solution is the eventual disappearance of silver peaks for longer milling experiments, featured in Figure 8.

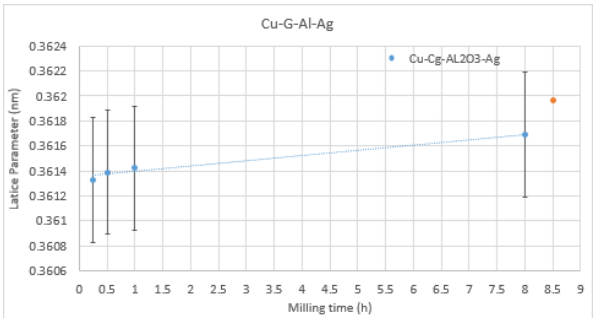

Figure 7 - Lattice parameter increase over time in the Cu-Cg-Al_2O_3-Ag system. The maximum lattice parameter shift for the used system, according to Vergard's law, is indicated.

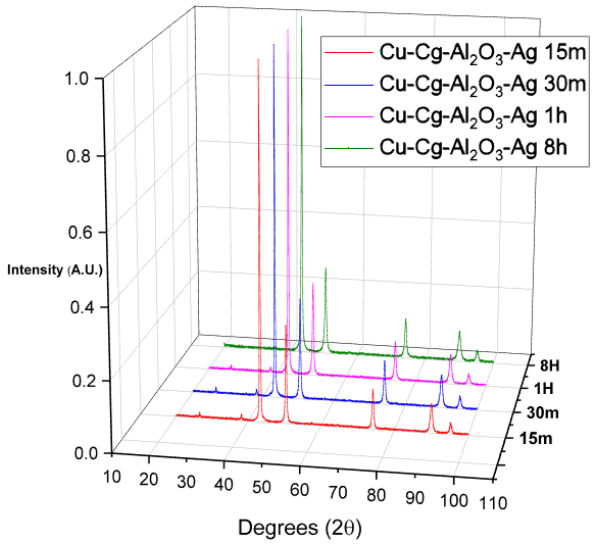

Figure 8 - X-ray diffractogram of milled powders in the Cu-Cg-Al_2O_3-Ag system

4.4. Scanning electron microscopy images

For short milling times, 15 min and 30 min, the average powder size seems very small in the order of 10μm. However, some huge grains can be found with sizes higher than 200 μm. These powders seem to contain small voids and cracks along the cross section. The smaller powders seem to be unwelded copper powders which maintain the initial powder size, in the order of 10-50μm. The big powders form from multiple welded powders with the voids and cracks displaying unwelded surfaces. Further milling for 1h reveals that most smaller powders have disappeared. The smaller powder size is now in the order of 20μm. Also, the previous big powders seem to have fractured at this point, as only powders in the order of 100 μm can be observed at this stage. This is indicative that powder cold working and fracture rate increases around 1h milling. Lastly, at 8 hours milling, no unwelded copper powders remain, and the welded agglomerates have fractured down, resulting in a

monomodal size distribution with an average grain size around 50 µm. Powders are almost void free, and the featured voids are big, resulting from the welding of a few big powders instead of the multiple small voids and cracks featured in 15 min and 30 min short milling times.

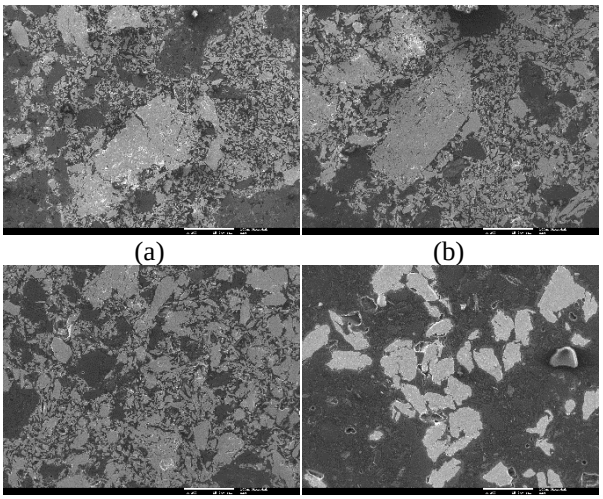

Figure 9 - SEM Micrograph of Cu-Cg milled powders after: a)15m milling b)30m milling c) 1h milling d) 8h milling. Scale bar = 100µm

As for powder morphology, in the 15 minute milling batch the smaller powders, with a small amount of welds, some retain the original dendritic shape, while the larger welded powders in the same batch have round shapes or flake like shapes and multiples welds, suggesting that the powder growth mechanism is deformation under impact resulting in cold welded powders.

The number of fractures and welds that develop under long milling times form layered flake like structures, with the welded interfaces visible. As powders get welded and flattened repeatedly, weld layer thickness decreases.

Welded powders in the 1 hour batches contain a large amount of voids which represent uncomplete welds, further milled powders in the 8h milling cycle are practically void free with the voids having origin in cold work fracture instead of unwelded surfaces.

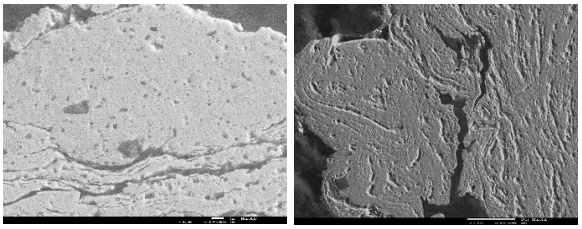

Figure 10 – Left) 30 Scale bar = 1µm; Right) 8h Scale bar= 10µm

SEM backscattered electrons images of both 30 min and 8 h milling, Figure 10, show graphite powders, and illustrate their successful dispersion inside copper grains, which is key in enabling the creation of a lubricating tribolayer [31].

4.5. Hardness testing

There are two main factors increasing the powder hardness when compared to the unmilled copper reference (80 HV).

The total matrix hardness can be interpreted as the cumulative hardness provided from all strengthening mechanisms [32]. The considered mechanisms are: the intrinsic copper lattice hardness, constant for all systems; work hardening of the copper matrix that can provide hardness increase up to 120HV [33]; Orowan strengthening - as milling progresses, reinforcement particles fracture and smaller dispersed particles are achieved, below 100nm, providing an obstacle do dislocation motion, and thus increasing composite hardness; Hall-Petch strengthening contributes to composite hardness due to decreasing crystallite size developed during milling; silver solid solution strengthening due to the increase of silver solubility in the copper structure along milling; second phase reinforcement, through a load sharing rule of mixtures, as hard dispersed particles act as a physical reinforcement of the composite.

Hardness increases due to the composite powder composition, as different powder additions either enable or increase an already present hardening mechanism. This increase can be observed when comparing the different systems. Hardness also increases along milling time, as longer milling times either enables or increase an already present mechanism. This increase can be observed when comparing the different milling time. All hardness measurements are reported on table 1.

The Cu-Cg 30m powder features a hardness of 179±18HV. The hardness contribution to this system can be divided into: intrinsic copper hardness (30HV) [34,35]; copper crystallite size hardening (26nm; 250HV) [34,35]; cold working of copper grains is expected to contribute with an hardness increase around 60 HV [33]; Orowan strengthening from dispersed graphite particles probably features a small contribution due to the initial particle diameter (d_{50}=2.4µm). This tentative estimation of powder hardness yields an expected hardness of 340 HV. While some values are overshoot, it indicates that, even for small milling times, the biggest contribution to composite hardness is grain size refinement.

Table 1 - Hardness measurements under ultra-microhardness testing

Milling time System	15min	30 min	1h	8h
System	Hardness Values (HV0.025)			
Reference Cu	84±6			
Cu-Cg	-	179±18	199±18	193±13
Cu-Cg-Al_2O_3	116±12	-	208+17	220±27
Cu-Cg-Al_2O_3-Ag	134±12	201±21	221±8	218±17

The Cu-Cg composite powders milled for 1 and 8 hours saw an increase in hardness. This hardness increase can be attributed to further refinement of the grain structure. The 8h composite, featuring the smallest crystallite mean size, does not display an hardness increase. A small decrease could even be ascertained, suggesting that a saturation harness was achieved.

The Cu-Cg-Al_2O_3 system enables two more hardening mechanisms beyond those active in the Cu-Cg system. The end result is a higher overall hardness for all milling times. Load sharing of alumina provides a maximum hardness increase around 4 HV, due to the small (4%) volume occupied by alumina particles inside the composite powders. Orowan strengthening provides the additional increase in comparison with the Cu-Cg system. Orowan strengthening is expected to increase along milling time: this effect is confirmed by the increasing hardness difference between the Cu-Cg and Cu-Cg-Al_2O_3 systems, which is 9 HV and 27 HV, respectively for 1h and 8h milling, despite a similar rate of crystallite size reduction.

The Cu-Cg-Al_2O_3-Ag system enables solid solution strengthening, this contribution is expected to increase along higher milling times, as solid solution during milling is an impact activated process. This effect is confirmed by the gradual increase in the lattice parameter along milling times reported in Figure 7. However, the biggest increase in the Cu-Cg-Al_2O_3-Ag in relation to Cu-Cg-Al_2O_3 system is found at 15m, suggesting that silver solid solution happens at short milling times and with significant increase (18HV).

5. Conclusions

Several experiments were carried out to produce contamination free copper composite powders using the synergic milling route. To avoid oxidation of the metal, powder processing and handling was carried out under a high purity Argon atmosphere with an Oxygen and H_2O content below 0,1 ppm. Powders were produced using 15m, 30m, 1h and 8h milling runs for various systems, with an increasing number of elements being added into the powder batch, respectively, Cu-Cg, Cu-Cg-Al_2O_3 and Cu-Cg-Al_2O_3-Ag. The compositions Cu-2wt%Cg, Cu-2wt%Cg-2wt%Al_2O_3, and Cu-2wt%Cg-2wt%Al_2O_3-1,6wt%Ag were selected.

The milling process efficiency was the main process bottleneck in the early stages of experimental procedure, with longer milling times resulting in low powder mass yield. Also, milling rates over 200 RPM, even for short time intervals, reduced process efficiency below the acceptable yield. This result was not observed in non-synergistic milling in air [20–22,36], and suggests that adhesion to the milling media and cold-welding is increased when working within oxide free synergic milling.

The use of 200 RPM milling rate featured an increase in process efficiency over an acceptable threshold for characterization for all milling times. However, the chief reason for process yield increase was the addition of silver to the powder batch, opening the possibility of enabling higher milling rates.

Electrolytic copper powders start with a dendritic shape. Through cold-welding the powders start growing and forming layered powders with a bimodal distribution, featuring both large sized welded powders and small unwelded powders. After 1 h milling, cold worked powders fracture and powder size becomes less inhomogeneous. At 8 h milling, compact like powders form. Average powder size grows over time during all milling runs.

Solid solution between copper and silver in mechanical milling increases composite hardness and reduces ductility. This effect changes powder mass transfer behaviour, increasing the process mass yield. Solid solution is difficult to characterize for low solute contents; however, x-ray diffraction shows the suppression of silver peaks and a lattice parameter increase, particularly from 1 hour to 8 hours milling. The additional change in composite properties, such as a hardness increase, and the change in mass transfer behaviour are indicative of a successful solid solution.

While alumina and silver additions increase the composite hardness, work hardening and crystallite size reduction appears to play a major role in hardness increase. However, silver additions are still relevant to provide composite performance and enable milling efficiency.

The production of MMC copper composites with graphite and alumina reinforcing phases and combinations thereof, as well as silver alloying was successful. A successful employment of the synergic milling approach to reduce contamination during milling and tackling the inherent challenges of synergic milling approach is reported. No contamination was found in the copper composites either by X-ray diffraction or EDS analysis. An increase in powder hardness is reported, with the

maximum value of 220 HV both in the Cu-Cg-Al_2O_3 and Cu-Cg-Al_2O_3-Ag systems. This result is far from the projected 300HV, but is nonetheless higher than the available values for work hardened copper, which shows that high energy milling is an effective method of increasing copper hardness by creating a nanostructured composite matrix [33] and is higher (or comparable in the case of systems with and higher alumina wt%) than most values previously reported for ODS copper via high energy mechanical milling [37–41].

6. Acknowledgements

The author is indebted to POMETON SPA, for supplying the Cu powder. This work was supported by FCT, Portugal under grants UID/CTM/04540/2019 and UIDB/04540/2020.

7. References

1. Nunes D, Correia JB, Carvalho PA, Shohoji N, Fernandes H, Silva C, et al. Production of Cu/diamond composites for first-wall heat sinks. Fusion Eng Des. 2011;86(9–11):2589–92.
2. Carvalho PA, Fonseca I, Marques MT, Correia JB, Almeida A, Vilar R. Characterization of copper-cementite nanocomposite produced by mechanical alloying. Acta Mater. 2005;53(4):967–76.
3. Decker F, Harker D. Recrystallization in rolled copper. Trans Aime. 1950;188(June):887–90.
4. Dias M, Antão F, Catarino N, Galatanu A, Galatanu M, Ferreira P, et al. Sintering and irradiation of copper-based high entropy alloys for nuclear fusion. Fusion Eng Des. 2019;146(March):1824–8.
5. Hussain Z, Kit LC. [1] Z. Hussain and L. C. Kit, “Materials & Design Properties and spot welding behaviour of copper – alumina composites through ball milling and mechanical alloying,” vol. 29, pp. 1311–1315, 2008.Materials & Design Properties and spot welding behaviour of . 2008;29:1311–5.
6. Braunovic M, Myshkin NK, Konchits V V., Myshkin NK, Konchits V V. Electrical Contacts: Fundamentals, Applications and Technology (Electrical and Computer Engineering). 2006;672.
7. Lee PK, Johnson JL. High-Current Brushes, Part II: Effects of Gases and Hydrocarbon Vapors. IEEE Trans Components, Hybrids, Manuf Technol. 1978;1(1):40–5.
8. Moustafa SF, El-badry SA, Sanad AM, Kieback B. Friction and wear of copper – graphite composites made with Cu-coated and uncoated graphite powders. Wear. 2002;253(7–8):699–710.
9. Moustafa SF, Ei-badry A. Effect of graphite with and without copper coating on consolidation behaviour and sintering of copper-graphite composite. Powder Metall. 1997;40(3):201–6.
10. Ying DY, Zhang DL. Processing of Cu – Al 2 O 3 metal matrix nanocomposite materials by using high energy ball milling. Mater Sci Eng. 2000;286(1):152–6.
11. ASM Handbook: Powder Metal Technologies and Applications. 9th ed. Vol. 7. 1988. 2148–2191 p.
12. Vitek JM, Warlimont H. The mechanism of anneal hardening in dilute copper alloys. Metall Trans A. 1979;10(12):1889–92.
13. Nestorovic S, Rangelov I, Markovic D, Nestorovic S, Rangelov I, Markovic D. Improvements in properties of sintered and cast Cu – Ag alloys by anneal hardening effect Improvements in properties of sintered and cast Cu – Ag alloys by anneal hardening effect. 2016;5899(April):35–9.
14. ASM International Handbook Committeee. ASM Speciality Handbook, Copper and Copper Alloys. 2001. 35–54 p.
15. Kang N, Coddet P, Liao H, Coddet C. Cold gas dynamic spraying of a novel micro-alloyed copper: Microstructure, mechanical properties. J Alloys Compd. 2016;686:399–406.
16. © Copper Development Association. Effect of various elements (impurities or intentional additions) on the conductivity of copper. 2018.
17. Suryanarayana C. Mechanical alloying and milling. Prog Mater Sci. 2001;46(1–2):1–184.
18. Eckert J, Holzer JC, Krill CE, Johnson WL. Structural and thermodynamic properties of nanocrystalline fcc metals prepared by mechanical attrition. J Mater Res. 1992;7(7):1751–61.
19. Koch CC. Synthesis of nanostructured materials by mechanical milling: Problems and opportunities. Nanostructured Mater. 1997;9(1–8):13–22.
20. Madavali B, Lee JH, Lee JK, Cho KY, Challapalli S, Hong SJ. Effects of atmosphere and milling time on the coarsening of copper powders during mechanical milling. Powder Technol. 2014;256:251–6.
21. Shukla AK, Nayan N, Murty SVSN, Mondal K, Sharma SC, George KM, et al. Processing copper-carbon nanotube composite powders by high energy milling. Mater Charact. 2013;84:58–66.
22. Zhang DL, Raynova S, Koch CC, Scattergood RO, Youssef KM. Consolidation of a Cu-2.5 vol.% Al2O3 powder using high energy mechanical milling. Mater Sci Eng A. 2005;410–411:375–80.
23. Tuinstra F, Koenig JL. Raman Spectrum of Graphite. J Chem Phys. 1970;53(3):1126–30.

24. Schwan J, Ulrich S, Batori V, Ehrhardt H, Silva SRP. Raman spectroscopy on amorphous carbon films. J Appl Phys. 1996;80(1):440–7.
25. Welham NJ, Berbenni V, Chapman PG. Effect of extended ball milling on graphite. J Alloys Compd. 2003;349(1–2):255–63.
26. Shen TD, Koch CC. Influence of dislocation structure on formation of nanocrystals by mechanical attrition. Mater Sci Forum. 1995;179–181:17–24.
27. Hellstern E, Fecht HJ, Fu Z, Johnson WL. Structural and thermodynamic properties of heavily mechanically deformed Ru and AlRu. J Appl Phys. 1989;65(1):305–10.
28. Eckert J, Holzer JC, Krill CE, Johnson WL. Mechanically driven alloying and grain size changes in nanocrystalline Fe-Cu powders. J Appl Phys. 1993;73(6):2794–802.
29. Uenishi K, Kobayashi KF. Formation of a super-saturated solid solution in the Ag-Cu system by mechanical alloying. Mater Sci Eng. 1991;134:1342–5.
30. Eckert J, Holzer JC, Krill CE, Johnson WL. Reversible grain size changes in ball-milled nanocrystalline Fe—Cu alloys. J Mater Res. 1992;7(8):1980–3.
31. Kováčik J, Emmer Š, Bielek J, Keleši L. Effect of composition on friction coefficient of Cu-graphite composites. Wear. 2008;265(3–4):417–21.
32. Kim WJ, Park IB, Han SH. Formation of a nanocomposite-like microstructure in Mg-6Al-1Zn alloy. Scr Mater. 2012;66(8):590–3.
33. Thompson JG. Effects of cold-rolling on the indentation hardness of copper. J Res Natl Bur Stand (1934). 1934;13(5):745.
34. Nunes D. Carbon dispersions in nanostructured metals. Instituto Superior Técnico; 2012.
35. Taha AS, Hammad FH. Application of the Hall-Petch Relation to Microhardness Measurements on Al, Cu, Al-MD 105, and Al-Cu Alloys. Phys Status Solidi. 1990;119(2):455–62.
36. Seixas T. Development and modeling of mechanical alloying for production of copper matrix composite powders reinforced with alumina and graphite. Instituto Superior Técnico; 2016.
37. Zhou D, Zhang D, Kong C, Munroe P, Torrens R. Grain and nanoparticle coarsening of an ultrafine structured Cu-5 vol.%Al2O3 nanocomposite during isochronal annealing. J Alloys Compd. 2015;642:83–91.
38. Rajković V, Erić O, Božić D, Mitkov M, Romhanji E. Characterization of dispersion strengthened copper with 3wt%Al 2 O 3 by mechanical alloying. Sci Sinter. 2004;36(3):205–11.
39. Rajkovic V, Bozic D, Popovic M, Jovanovic MT. The influence of powder particle size on properties of Cu-Al 2O3 composites. Sci Sinter. 2009;41(2):185–92.
40. Rajkovic V, Romhanji E, Mitkov M. Characterization of high-energy ball milled prealloyed copper powder containing 2.5 wt%Al. J Mater Sci Lett. 2002;21(2):169–73.
41. Yan P, Lin C, Cui S, Lu Y, Zhou Z, Li Z. Microstructural features and properties of high-hardness and heat-resistant dispersion strengthened copper by reaction milling. J Wuhan Univ Technol Mater Sci Ed. 2011;26(5):902–7.